COMSOL CONFERENCE 2024 FLORENCE

Developing 2D and 3D micropolar FEM models for porous GBR meshes in dentistry applications

A.M. Rezaei[1], R. Izadi[1], N. Fantuzzi[2]
1. Sapienza University of Rome, Rome, RM, Italy.
2. University of Bologna, Bologna, BO, Italy.

Abstract
In the present work, COMSOL® Multiphysics is used to implement 2D and 3D micropolar continuum models to address the multidisciplinary problem of modelling guided bone regeneration (GBR) meshes. GBR meshes are used in dentistry as mechanical barriers to isolate and protect the area of bone loss from the surrounding tissue while allowing for new bone growth. The micropolar theory is adopted to provide a homogenised and efficient mechanical model for the heterogeneous porous structure of the GBR mesh. The mechanical constants are derived based on the strain energy equivalence between a periodic porous plate and its equivalent micropolar model under prescribed boundary conditions. The effects of various architectural features, such as pore shapes, patterns, and sizes, on the material parameters are investigated. The results show that the micropolar theory can effectively predict the mechanical response of the GBR mesh with a more reliable performance compared to the classical Cauchy theory. The collected equivalent micropolar parameters are further used for GBR mesh design, considering both mechanical and biomedical requirements. As an example, different materials and arrangements are analysed to find micropolar constitutive parameters that are comparable to bone parameters reported in the literature. This allows the GBR mesh to possess the mechanical performance that matches the adjacent bones and avoid the stress-shielding phenomenon.
Keywords: Guided Bone Regeneration; COMSOL® Multiphysics; Micropolar Theory; Finite Element Analysis; Equivalent Porous-Cellular Materials.

Introduction
Bone tissue has a limited capacity for self-repair and cannot regenerate if the damaged area is too large. To support cellular proliferation and facilitate the filling of the damaged region, scaffolds are commonly employed [1], [2], [3]. These scaffolds are porous structures made from biomaterials, designed to provide mechanical support and encourage bone regeneration [4]. Guided Bone Regeneration (GBR) is a dental surgical procedure (see Figure 1) used to regenerate bone in specific areas where natural bone volume is insufficient, often in preparation for dental implants. The effectiveness of GBR depends significantly on the mechanical properties of the barriers [5]. The primary function of the scaffolds is to preserve the tissue while transferring appropriate mechanical forces [2]. The bone regrowth is dependent on the mechanical forces experienced by regenerating cells. Ideally, bone scaffold should mimic the stiffness of natural bone [6] as close as possible. On the other hand, studies suggest that the intricate structure of bone tissue may require more sophisticated mechanical models, such as micropolar theory, to take into account the effect of internal structures [7]. At the same time, compromising porosity and stiffness is crucial, as increasing porosity reduces stiffness but supports nutrient flow, waste removal, and cell migration [8]. As another challenge, metallic GBR sheets that are currently used as mechanical barriers (Figure 1***d***) should be removed after the healing period, which imposes a second surgery for the patients. To eliminate the need for this second procedure, a solution is to use biodegradable materials like polylactic acid (PLA) [9].

Figure 1. Guided bone regeneration surgical procedure: ***a)*** *Exposing the Bone Defect: A small incision is made so to access the area of defect.* ***b)*** *Bone Grafting: a cement (bone+antimicrobial additives+stimulants) that promotes new bone growth is placed under the membrane.* ***c)*** *Preparing GBR Mesh:* ***d)*** *Placing the GBR Mesh*

The use of biodegradable material is also of great desire due to the recent advances in additive manufacturing, which enable the production of highly precise and customised 3D scaffolds with

tuneable pore size, density, and architecture. This allows for optimisation of their mechanical and biological performance by tailoring microstructural characteristics. However, biodegradable polymers such as PLA usually possess suboptimal mechanical properties, such as low stiffness and fracture toughness, that limit their application and there is the need to use reinforcements [10], [11].

The current work attempts to address the multifaceted and multidisciplinary challenges in the design of the GBR implants by proposing a mechanical model that can efficiently consider the effect of material and microstructure on the overall behaviour. The model is based on the micropolar theory, which considers the effect of internal structure through internal scale parameters in the equations [12]. This mechanical model will facilitate the design of GBR implants that can replicate the mechanical properties of that of the natural bone.

The 2D and 3D governing equations of micropolar theory are implemented using the PDE Weak form in COMSOL® to conduct FE simulations. The developed implementation can account for complex geometry, loading and boundary conditions within a user-friendly interface. Also, the visualisation of the results and postprocessing will be quite convenient.

Theoretical Background

3D Micropolar Theory

In classical continuum mechanics, materials are modelled as continuous entities without internal structure, leading to the assumption that the stress tensor is symmetric. However, this assumption fails in materials where microstructural effects play a significant role. Micropolar (or Cosserat [13]) continuum theory addresses this limitation by introducing additional kinematic variables.

In this theory, a microscopic rotational degree of freedom, called micro-rotation (Φ), is considered besides the usual translational deformations (U) in classical (Cauchy) continua.

This continuum is governed by the following linearised kinematic equations [14]:

$$\begin{aligned} E_{ij} &= U_{j,i} - e_{ijk}\Phi_k \\ K_{ij} &= \Phi_{j,i} \end{aligned} \tag{1}$$

where U and Φ stand for the displacement and micro-rotation vectors, E_{ij} and K_{ij} denote the components of strain and curvature tensors and e_{ijk} is the usual third order permutation symbol.

If the presence of body forces (P_j) and body couples (Q_j), the equilibrium equations take the following form:

$$\begin{aligned} \Sigma_{ij,i} + P_j &= 0 \\ M_{ij,i} - e_{ijk}\Sigma_{ik} + Q_j &= 0 \end{aligned} \tag{2}$$

Where Σ_{ij} and M_{ij} are the non-symmetric stress and couple-stress tensors, respectively.

In the isotropic micropolar solid there are six elastic constants, in contrast to the two parameters in the classical elastic solid. The constitutive equations are:

$$\begin{aligned} \Sigma_{ij} &= \lambda E_{kk}\delta_{ij} + \mu E_{ji} + (\mu+\kappa)E_{ij} \\ M_{ij} &= \alpha K_{kk}\delta_{ij} + \beta K_{ji} + \gamma K_{ij} \end{aligned} \tag{3}$$

Eq. (3) includes six elastic material constants: the two Lamé's constants, λ and μ , similar to Cauchy continua plus four extra parameters, α , β , γ , κ , related to the micropolar theory. The engineering constants listed below (Table 1) can be derived from these six constitutive parameters, providing a more sensible understanding of the physical properties [14]:

Table 1: Engineering constants for a linear isotropic micropolar elastic

(Generalised) Shear Modulus	$G = \mu + \frac{\kappa}{2}$
(Generalised) Young's Modulus	$E = \frac{(2\mu+\kappa)(3\lambda+2\mu+\kappa)}{2\lambda+2\mu+\kappa}$
(Generalised) Poisson Ratio	$\nu = \frac{\lambda}{2\lambda+2\mu+\kappa}$
Characteristic Length for Torsion	$l_t = \sqrt{\frac{\beta+\gamma}{2\mu+\kappa}}$
Characteristic Length for Bending	$l_b = \sqrt{\frac{\gamma}{2(2\mu+\kappa)}}$
Polar Ratio	$\psi = \frac{\beta+\gamma}{\alpha+\beta+\gamma}$
Coupling Number	$N = \sqrt{\frac{\kappa}{2(\mu+\kappa)}}$

Micropolar Theory in 2D Plane

In the linearised 2D framework of micropolar, the degrees of freedom are reduced to two displacements (U , V) and one rotational component (Φ), so the generalised displacement vector can be defined as:

$$\mathbf{U}^{\mathrm{T}} = \{U \quad V \quad \Phi\} \tag{4}$$

and the strain vector is:

$$\mathbf{E}^{T} = \{E_{11} \quad E_{22} \quad E_{12} \quad E_{21} \quad K_1 \quad K_2\} \tag{5}$$

Where E_{11} , E_{22} , E_{12} , E_{21} are the in-plane normal and shear strains, and K_1 , K_2 are the micropolar curvatures that exist in the plane.

The stress vector is also represented as:

$$\mathbf{\Sigma}^{T} = \{\Sigma_{11} \quad \Sigma_{22} \quad \Sigma_{12} \quad \Sigma_{21} \quad M_1 \quad M_2\} \tag{6}$$

where Σ_{ij} $(i, j = 1,2)$ represents the normal $(i = j)$ and shear stress $(i \neq j)$ components, and M_1 , M_2 are the micro-couples act in-plane.

The general micropolar anisotropic constitutive equations can be represented as:

$$\boldsymbol{\Sigma} = \mathbf{C}\mathbf{E} \tag{7}$$

Where **C** is the symmetrical constitutive stiffness matrix. Accordingly, Eq. (7) can be written in terms of the stiffness matrix components and Voigt notation as:

$$\begin{Bmatrix} \Sigma_{11} \\ \Sigma_{22} \\ \Sigma_{12} \\ \Sigma_{21} \\ M_1 \\ M_2 \end{Bmatrix} = \begin{bmatrix} A_{1111} & A_{1122} & A_{1112} & A_{1121} & B_{111} & B_{112} \\ & A_{2222} & A_{2212} & A_{2221} & B_{221} & B_{222} \\ & & A_{1212} & A_{1221} & B_{121} & B_{122} \\ & & A_{1221} & A_{1212} & B_{221} & B_{212} \\ & & & & D_{11} & D_{12} \\ sym. & & & & & D_{22} \end{bmatrix} \begin{Bmatrix} E_{11} \\ E_{22} \\ E_{12} \\ E_{21} \\ K_1 \\ K_2 \end{Bmatrix} \tag{8}$$

The geometries considered here for porous GBR meshes (Figure 3) are symmetric with respect to a 90° rotation. This symmetry implies a special kind of orthotropic material known as "ortho-tetragonal." The constitutive equations for materials with ortho-tetragonal symmetry can be presented as:

$$\begin{Bmatrix} \Sigma_{11} \\ \Sigma_{22} \\ \Sigma_{12} \\ \Sigma_{21} \\ M_1 \\ M_2 \end{Bmatrix} = \begin{bmatrix} A_{1111} & A_{1122} & 0 & 0 & 0 & 0 \\ A_{1122} & A_{1111} & 0 & 0 & 0 & 0 \\ 0 & 0 & A_{1212} & A_{1221} & 0 & 0 \\ 0 & 0 & A_{1221} & A_{1212} & 0 & 0 \\ 0 & 0 & 0 & 0 & D_{11} & 0 \\ 0 & 0 & 0 & 0 & 0 & D_{11} \end{bmatrix} \begin{Bmatrix} E_{11} \\ E_{22} \\ E_{12} \\ E_{21} \\ K_1 \\ K_2 \end{Bmatrix} \tag{9}$$

Therefore, the stiffness matrix contains five independent micropolar material parameters: A_{1111}, A_{1122}, A_{1212}, A_{1221}, D_{11}.

Methods

2D Plate Model for Porous GBR Mesh

Currently, there are several types of GBR mesh available on the market. A common type that is widely used in dentistry is titanium alloy (Ti6Al4V) [15] sheets with a perforated structure. Before implantation of the GBR, the required dimensions and overall shape are cut and formed by the surgeon (Figure 1***c***).

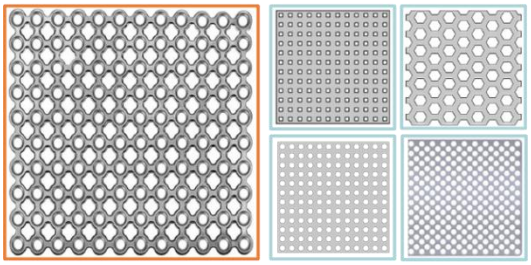

Figure 2 Different pore geometries and patterns considered for GBR meshes.

GBR meshes are considered here as 2D square plates with an overall side length of L where pores are distributed regularly. The pores can be in various shapes and sizes and with different spacing, which leads to different pore densities. Here, the pores' geometry and pattern are parametrised by two variables, the pore size, l_p and the number of pores per unit length (pore density), N_p. The parametrised GBR sheets with rectangular- and circular-shape pores are shown in Figure 3.

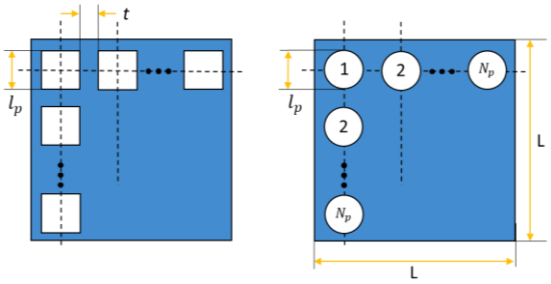

Figure 3 Parametrised GBR sheet with rectangular and circular shape pores

Homogenisation and Identification of Micropolar Parameters for 2D Plate

For modelling the GBR meshes with different microstructures (pores' patterns), an equivalent homogenised material represents the detailed heterogeneous structure. At the macro-level, the micropolar continuum is chosen as it has been shown to be very suitable to describe materials with internal structures, while at the micro-level the classical Cauchy continuum is used (Figure 4).

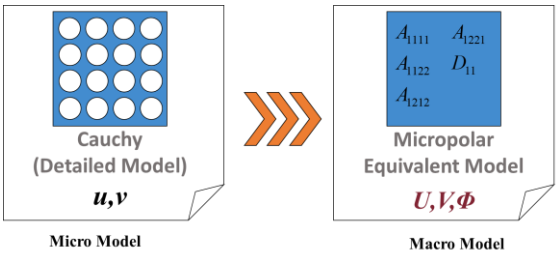

Figure 4 The homogenisation procedure for 2D model of porous GBR meshes.

To determine the constitutive parameters of the equivalent model, the primary hypothesis is that the strain energy stored in the porous structure under prescribed boundary conditions is equal to that of the equivalent continuum description. First, we calculate the response of the porous plate subjected to various loadings using FE analysis by COMSOL®. Then, for each case, the corresponding micropolar material parameters are found so that the equivalent material stores the same total strain energy when subjected to the identical loading. The details of the homogenisation procedure can be found in [16]. Also, for the more general case of orthotropic pore configurations, the procedure described in [17] can be followed.

3D Model for Porous GBR Scaffold

Beside the 2D GBR membrane introduced and modelled in the previous section, the 3D bio-inspired microstructures such as gyroids and other triply periodic minimal surfaces (TPMS) (Figure 5) can be employed for designing GBR scaffolds.

Homogenised 3D micropolar theory can be utilised to model various microstructure topologies and distributions.

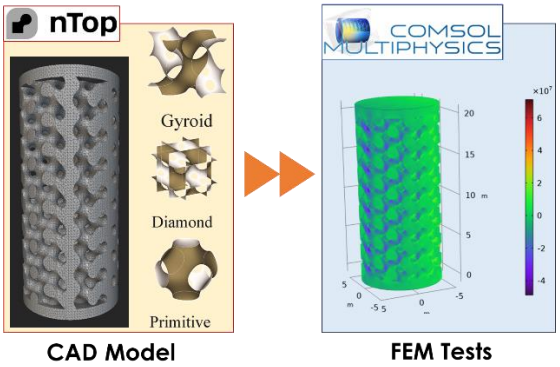

Figure 5 Meta material modelling in nTop and FE analysis in COMSOL on the imported meshed geometry.

Homogenisation and Identification of Micropolar Parameters in 3D Model

Although the methodology presented for the 2D model can be extended for the 3D problem, to present a different idea, the size dependency observed in the torsional stiffness of the metamaterial is utilised to find the micropolar material parameters.

For micropolar elastic materials, a size effect is predicted in the torsion and bending of circular cylinders that differentiate them from classical (Cauchy) theory description [18].

In micropolar media, thin and slender rods are more rigid than would be expected classically [19]. More precisely, the ratio of torsional rigidity (torsional stiffness) of a micropolar cylinder of radius R to its classical value is shown to be [14]:

$$\Omega_T = \frac{K_{T,micropoalr}}{K_{T,classsical}} = 1 + 6\left(\frac{l_t}{R}\right)^2 \frac{1-\frac{4}{3}\psi X}{1-\psi X} \qquad (10)$$

In which $K_{T,classsical}$ is the torsional rigidity (the torque required to produce unit angle of twist) and defined as the product of the shear modulus (G) and polar moment of inertia (J). Also,

$$X = \frac{I_1(pR)}{pRI_0(pR)}$$
$$p = \sqrt{\frac{2\kappa}{(\alpha+\beta+\gamma)}} \qquad (11)$$

Where I_0 and I_1 are the modified Bessel functions of the first kind of order 0 and 1, respectively.

From Eq. (10), it is clear that for micropolar bodies, $\Omega_T \geq 1$ and the torsional rigidity is higher than what is expected classically and reveals the occurrence of the "size effect", which is more dominant in smaller diameters, where the internal length becomes comparable to cylinder diameter [14].

The equivalent micropolar parameters of the scaffolds will be found using numerical simulations for torsion deformations at different length scales. In this method, a set of numerical FE simulations is conducted on cylinders with different diameters while keeping the microstructure (unit cell size) constant (Figure 6).

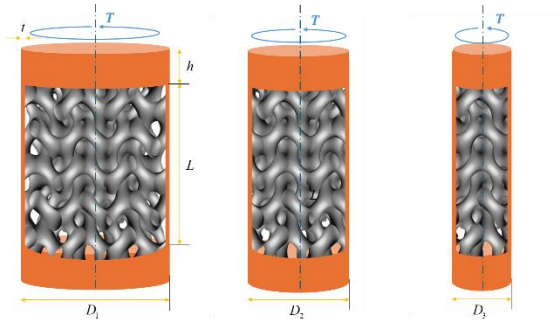

Figure 6 Numerical simulations for torsion deformations at different length scales while keeping unit cell size.

The torsional rigidities obtained from FE simulations and the continuum relations of Eq.s (10) and (11) will be incorporated through an optimisation approach to determine the micropolar parameters.

Simulation

The detailed porous structures and the equivalent micropolar models in 2D and 3D were simulated by using COMSOL®. For 3D modelling of the metamaterials, nTop® was used. In this software, the TPMS microstructures are already available and easily customisable to produce efficient meshed models of the sample.

2D and 3D FE Micropolar Models in COMSOL®

To implement the micropolar theory numerically for solids, we used the capability of COMSOL® Multiphysics to apply the weak form to partial differential equations (PDE). The micropolar theory or other non-classical continua is not yet available in commercial FE codes. By using PDE modelling in COMSOL®, no user subroutines are required, and various complex geometries, boundary conditions, and loadings can be applied in a user-friendly graphical interface. Also, the visualisation of the results and obtaining the required data from FEM analysis is quite convenient. Building such a multi-purpose and flexible model where the base material is a micropolar continuum is not straightforward when coding from scratch or using other FEM packages [20].

To develop the weak form, we multiply each of the balance equations in Eq. (2) by the test functions corresponding to unknowns U_i and Φ_i , denoted here as v_U and v_Φ , and integrate over the entire computational domain *D:*

$$\int_D \Sigma_{ij,i} v_{U_j} + \int_D P_j v_{U_j} = 0$$
$$\int_D M_{ij,i} v_{\Phi_j} - \int_D e_{ijk}\Sigma_{ik} v_{\Phi_j} + \int_D Q_j v_{\Phi_j} = 0 \qquad (12)$$

Then, based on the product rule of derivatives, we have:

$$\int_D \Sigma_{ij,i} v_{U_j} = \int_D \left(\Sigma_{ij} v_{U_j}\right)_{,i} - \int_D \left(\Sigma_{ij} v_{U_{j,i}}\right)$$
$$\int_D M_{ij,i} v_{\Phi_j} = \int_D \left(M_{ij} v_{\Phi_j}\right)_{,i} - \int_D \left(M_{ij} v_{\Phi_{j,i}}\right) \quad (13)$$

And by using the divergence theorem and considering B as the surface boundary surrounding this domain, the weak form PDE for the momentum and angular momentum balance can be defined:

$$-\int_D \Sigma_{ij} v_{U_{j,i}} + \int_B \Sigma_{ij} v_{U_j} n_i + \int_D P_j v_{U_j} = 0 \quad (14)$$
$$-\int_D M_{ij} v_{\Phi_{j,i}} + \int_B M_{ij} v_{\Phi_j} n_i - \int_D e_{ijk} \Sigma_{ik} v_{\Phi_j} + \int_D Q_j v_{\Phi_j} = 0$$

For the equivalent micropolar models, first-order (linear) elements (for both displacements and micro-rotation) are used for discretisation of 2D and 3D domains.

Validation of micropolar FE models

The developed FEM micropolar models in 2D and 3D were tested with the available benchmarks from the literature. For instance, the results of the patch test introduced in [21] for 2D and in [22] for 3D were consistent with the analytical solutions reported there as benchmark values.

Results and Discussion

Prediction of mechanical behaviour by micropolar theory

To evaluate the capability of the developed micropolar model to predict the mechanical response, the indentation of a vertical load on a porous plate (Figure 7) was investigated for both circular and square pores with different pore sizes.

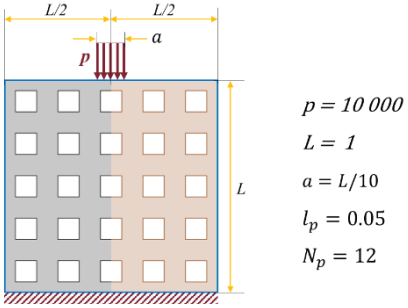

Figure 7 The geometry, loading and boundary conditions to evaluate the homogenised micropolar model.

For instance, the magnitude of the displacement for the real porous structure and the homogenised micropolar and Cauchy models are shown in Figure 8 for square pores of size 0.05L. The values of the displacements are labelled on the corresponding contour lines.

As can be seen, the prediction of the micropolar theory is closer to the real porous structure, and the load penetration reflected in the displacement contours is better captured by the micropolar model.

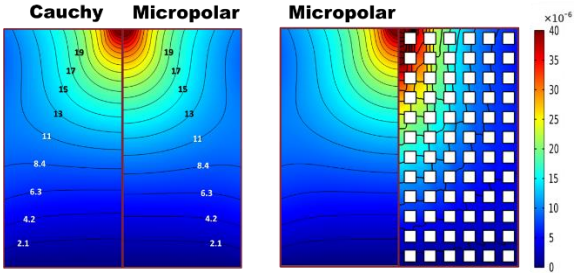

Figure 8 The comparison of displacement magnitude for the homogenised micropolar and Cauchy models with the detailed porous structure for square pores.

Designing porous GBR meshes

Bone is a heterogeneous material composed of microscopic units, including collagen fibrils and hydroxyapatite crystals, which influence its macroscopic mechanical properties. As pointed out earlier, the micropolar theory is capable of accounting for the size effects that are observed in the bone [7].

Based on the available experimental data in the literature for the cortical bone (for instance, [23], [24]), the coefficients of the stiffness matrix can be found as presented in Table 2. These values are also marked by the yellow regions in Figure 9.

Table 2: Micropolar stiffness matrix components for bone

Parameter	Unit	Value
A_{1111}	GPa	12.00 ~ 43.43
A_{1122}	GPa	4.00
A_{1212}	GPa	21.10 ~ 36.77
A_{1221}	GPa	-13.05 ~ 2.67
D_{11}	kN	3.24

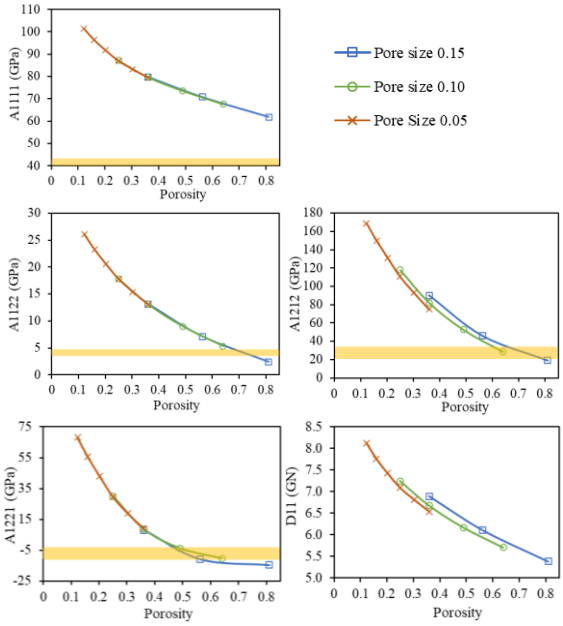

Figure 9 Equivalent micropolar parameters for square pores (each dataset for a specific pore size and various number of pores). The yellow area indicates the compact bone equivalent parameter range.

The results from the parametric study of GBR sheets (Figure 9) allow us to find a configuration with the material parameters close to the bone. For instance, in the case of rectangular pore patterns with a size of $0.13 \sim 0.15$ and porosity about 0.7, a good agreement for A_{1111} , A_{1122} and A_{1212} can be achieved.

FG Porous Design for GBR Mesh

The equivalent homogenised model for functionally graded (FG) porous structures can be derived by considering the homogenisation procedure developed for unit cells with uniform porosity (Figure 10). First, a parametric study is conducted to find the equivalent mechanical parameter of uniform porous plates with various pore sizes. In the parametric study, the pore sizes are changed to find the required equivalent parameters for each section of FG porous structure.

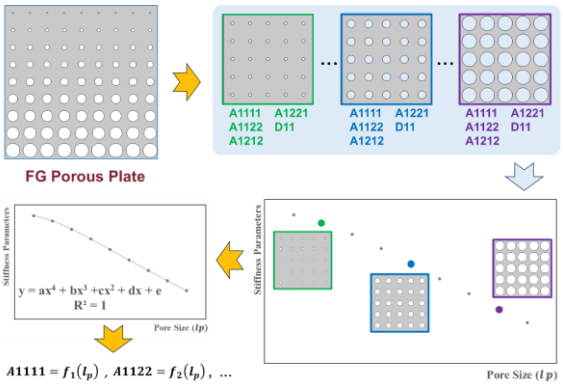

Figure 10 The methodology for developing equivalent homogenised models of FG porous plates

Being inspired by the natural functionally graded (FG) porous structure of the bone, a new design for GBR mesh can be suggested (Figure 11) so that the central part possesses mechanical properties close to cancellous (trabecular) bone while providing a proper porosity and the part near fixing areas (screw's location) as near as possible to cortical (compact) bone to provide required load-bearing capacities.

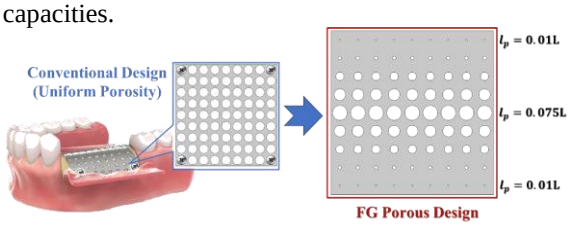

Figure 11 The suggested FG porous (Type O) design for GBR mesh

Designing FG 3D GBR scaffold

The developed methodology enables efficient investigation of functional grading (FG) in both topological and material characteristics. The changes in microstructural architecture and material constituents will be reflected in the spatial function of equivalent micropolar parameters. By implementing the developed model, we suggest an innovative design for FG 3D GBR scaffolds where the microstructure evolves from the highly porous structure inside the scaffold to the compact structure at the load-bearing surfaces to mimic the natural FG microstructure of the bone (Figure 12).

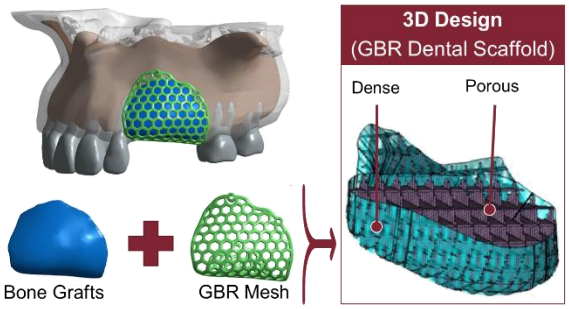

Figure 12 3D functionally graded design for GBR Meshes

A unified 3D design can simplify the surgery process and results in more precise bone regeneration. Also, it can be individualised for each patient and medical case.

Conclusions

In the current work, a multiscale method based on micropolar theory was developed to study and design the mechanical performance of GBR porous biomedical implants. Both 2D and 3D micropolar theories were implemented using the weak form of partial differential equations within COMSOL® Multiphysics, enabling handling of complex geometries and boundary conditions in a user-friendly interface.

The homogenisation procedure for the 2D framework was based on the equivalence of strain energy between the porous plate and the micropolar model under designed boundary conditions. In the 3D framework, the size-dependent behaviour observed in the torsional stiffness of porous cylinders was used to determine the equivalent micropolar model.

To demonstrate the applicability of this framework, it was employed to suggest the mechanical design of a functionally graded 2D GBR membrane providing mechanical performance closely aligned with that of the adjacent bone to avoid stress shielding. Besides, based on the developed framework, an innovative suggestion is proposed for the design of 3D GBR implants.

References

[1] D. J. Kelly and P. J. Prendergast, "Prediction of the Optimal Mechanical," *Tissue Eng*, pp. 2509-2519, 2006.

[2] A. Boccaccio, A. Ballini, C. Pappalettere, D. Tullo, S. Cantore and A. Desiate, "Finite Element Method (FEM), Mechanobiology and Biomimetic Scaffolds in Bone Tissue Engineering," *International Journal of Biological Sciences*, pp. 112-132, 2011.

[3] E. Sachlos and J. Czernuszka, "Making Tissue Engineering Scaffolds Work," *European Cells and Materials*, pp. 29-40, 2003.

[4] J. K. Griesbach, F. A. Schulte, G. N. Schädli, M. Rubert and R. Müller, "Mechanoregulation analysis of bone formation in tissue engineered constructs," *Acta Biomaterialia*, pp. 149-163, 2024.

[5] Z. Yang, C. Wu, H. Shi, X. Luo, H. Sun, Q. Wang and D. Zhang, "Advances in Barrier Membranes for Guided Bone Regeneration Techniques," *Frontiers in Bioengineering and Biotechnology*, vol. 10, 2022.

[6] A. Persaud, A. Maus, L. Strait and D. Zhu, "3D Bioprinting with Live Cells," *Engineered Regeneration*, vol. 3, pp. 292-309, 2022.

[7] M. Marin, E. Carrera and A. E. Abouelregal, "Structural stability study for porous Cosserat media," *Mechanics of Advanced Materials and Structures*, pp. 1-9, 2023.

[8] P. Gentile, V. Chiono, I. Carmagnola and P. Hatton, "An Overview of Poly(lactic-co-glycolic) Acid (PLGA)-Based Biomaterials for Bone Tissue Engineering," *International Journal of Molecular Sciences*, pp. 3640-3659, 2014.

[9] R. Izadi, M. Tuna, P. Trovalusci and N. Fantuzzi, "Thermomechanical characteristics of green nanofibers made from polylactic acid: An insight into tensile behavior via molecular dynamics simulation," *Mechanics of Materials*, vol. 181, 2023.

[10] R. Izadi, R. Das, N. Fantuzzi and P. Trovalusci, "Fracture properties of green nano fibrous network with random and aligned fiber distribution: A hierarchical molecular dynamics and peridynamics approach," *International Journal of Engineering Science*, vol. 204, p. 104136, 2024.

[11] R. Izadi, P. Trovalusci and N. Fantuzzi, "A Study on the Effect of Doping Metallic Nanoparticles on Fracture Properties of Polylactic Acid Nanofibres via Molecular Dynamics Simulation," *Nanomaterials*, vol. 13, p. 989, 2023.

[12] B. Niu and J. Yan, "A new micromechanical approach of micropolar continuum modeling for 2-D periodic cellular material," *Acta Mechanica Sinica/Lixue Xuebao*, vol. 32, pp. 456-468, 2016.

[13] E. M. P. Cosserat and F. Cosserat, Théorie des corps déformables, A. Hermann et fils, 1909.

[14] R. Izadi, M. Tuna, P. Trovalusci and E. Ghavanloo, "Torsional characteristics of carbon nanotubes: Micropolar elasticity models and molecular dynamics simulation," *Nanomaterials*, vol. 11, pp. 1-20, 2021.

[15] L. Bai, P. Ji, X. Li, H. Gao, L. Li and C. Wang, "Mechanical Characterization of 3D-Printed Individualized Ti-Mesh (Membrane) for Alveolar Bone Defects.," *Journal of healthcare engineering*, p. 4231872, 2019.

[16] A. Rezaei, R. Izadi and N. Fantuzzi, "Equivalent micropolar model for porous guided bone regeneration mesh: Optimum design for desired mechanical properties," *Applied Mathematical Modelling*, vol. 131, pp. 737-763, 2024.

[17] A. Rezaei, R. Izadi and N. Fantuzzi, "A Hierarchical Nano to Micro Scale Modelling of 3D Printed Nano-Reinforced Polylactic Acid: Micropolar Modelling and Molecular Dynamics Simulation," *Nanomaterials*, vol. 14, p. 1113, 2024.

[18] R. Izadi, M. Tuna, P. Trovalusci and N. Fantuzzi, "Bending characteristics of carbon nanotubes: Micropolar elasticity models and molecular dynamics simulations," *Mechanics of Advanced Materials and Structures*, vol. 30, pp. 189-206, 2021.

[19] R. D. Gauthier and W. E. Jahsman, "A Quest for Micropolar Elastic Constants," *Journal of Applied Mechanics*, pp. 369-374, 1975.

[20] A. Molavizadeh and A. Rezaei, "Progressive Damage Analysis and Optimization of Winding Angle and Geometry for a Composite Pressure Hull Wound Using Geodesic and Planar Patterns," *Applied Composite Materials*, 2019.

[21] E. Providas and M. Kattis, "Finite element method in plane Cosserat elasticity," *Computers & Structures*, vol. 80, pp. 2059-2069, 2002.

[22] S. Bauer, M. Schäfer, P. Grammenoudis and C. Tsakmakis, "Three-dimensional finite elements for large deformation micropolar elasticity," *Computer Methods in Applied Mechanics and Engineering*, pp. 2643-2654, 2010.

[23] J. Yang and R. S. Lakes, "Experimental study of micropolar and couple stress elasticity in compact bone in bending," *Journal of Biomechanics*, vol. 15, pp. 91-98, 1982.

[24] V. A. Eremeyev, A. Skrzat and F. Stachowicz, "Linear Micropolar Elasticity Analysis of Stresses in Bones Under Static Loads," *Strength of Materials*, pp. 575-585, 2017.